



## The Dynamic System of Funicular Train on Constant Railway Gradient with Controlled Water Discharge for Adaptive Braking System

Bagus Wahyudi<sup>1\*</sup>, Pipit Wahyu Nugroho<sup>1</sup>, Akhmad Faizin<sup>1</sup>, Hangga Wicaksono<sup>1</sup>, Safian Sharif<sup>2</sup>,  
Mohd Azlan Suhaimi<sup>2</sup>, Nur Safwati Mohd Nor<sup>2</sup>

<sup>1</sup> Mechanical Engineering Department, State Polytechnic of Malang, Kota Malang 65141, Indonesia

<sup>2</sup> Faculty of Mechanical Engineering, Universiti Teknologi Malaysia, Johor Bahru 81310, Malaysia

Corresponding Author Email: [bagus.wahyudi@polinema.ac.id](mailto:bagus.wahyudi@polinema.ac.id)

Copyright: ©2025 The authors. This article is published by IIETA and is licensed under the CC BY 4.0 license (<http://creativecommons.org/licenses/by/4.0/>).

<https://doi.org/10.18280/mmep.120108>

### ABSTRACT

**Received:** 22 October 2024

**Revised:** 18 December 2024

**Accepted:** 26 December 2024

**Available online:** 25 January 2025

#### Keywords:

*funicular train, water mass controlled, constant railway gradient, adaptive brake*

The purpose of this study is mainly to discuss mathematical modelling and simulation of a funicular train with water mass controlled. The funicular train carriage is equipped with a water reservoir, when the train goes up the water reservoir is empty and when the train goes down the reservoir is full. During the train's journey down the train carriage spills water continuously and in steady flow so that when it reaches the lower station the water reservoir will be empty. This study compares the performance of the car suspension system of the funicular train carriage when moving up and when moving down. The performance is then compared between traditional car model with water mass controlled provides better features in terms of ride quality and control. Mathematical modelling is developed and differential equations of motion are derived from a quarter car model. The equation is derived from knowing the response of the spring-mass movement due to the unsteady flow of water discharge on the descending vehicle carrying the mass of water in the tank as its driver. The mass of water the train carries is in full condition when it is going down and will run out on time when the train reaches the lower station. Water mass controlled provides ride quality and load distribution as same as traditional car model in sinusoidal loading mode simulations. The differential equations are solved with the help of computer simulation using MATLAB Simulink. The results include the displacement and acceleration of damped and undamped masses after hitting the rail joint bumps as well as the results of the system stability analysis. By simulated using a bump profile has almost the same value in a rise time of around 0.2-0.3 seconds, a maximum amplitude of around 0.2 m, a peak amplitude of around 0.22 m and a steady state of around 5.2 seconds.

## 1. INTRODUCTION

The focus on green transportation has grown significantly among global researchers due to the depletion of fossil fuel reserves and the escalating emissions of vehicle exhaust gases, leading to environmental pollution. According to a study by Nam et al. [1], transitioning to a train-based transportation system could potentially reduce overall emissions by up to 70%. Similarly, as noted by Albertus [2], trains play a vital role in boosting tourist visits in the East Java area, particularly following a decline in visitors due to the COVID-19 pandemic. This article aims to explore an environmentally friendly train transportation model that operates on the earth's gravity system, eliminating the need for fossil fuels and electricity. This type of train, akin to the Funicular Cable Car popular in Switzerland, is especially well-suited for providing tourist transportation in valleys or hilly areas with rail lines featuring extreme up or down slopes.

A funicular typically consists of two carriages on rails connected to opposite sides of a steel towing rope. As one carriage ascends, the other descends, and then the rope

reverses direction for the next cycle, requiring a lifting force known as "jig-back." This design is less rigid than using paired carriages. Some funiculars feature only one carriage with the towing rope not enclosed in a loop wound on a drum. In many countries, automatic funiculars with a single operator are also allowed to be used.

Modern funiculars are capable of running on both concave and convex tracks, as well as bending to the left and right. They are equipped with devices that ensure the train floor remains horizontal even on steep inclines and can adapt to significant changes in the track gradient. However, it's important to note that there are limitations to the track length, as the capacity of the jig-back system decreases with longer tracks, particularly those exceeding 2 or 3 km, which is crucial for safety.

The energy required varies along the line, but its efficiency is consistently better than that of a bus system connecting the same points with the same capacity, even under less severe traffic conditions. Essentially, an inclined elevator is a light funicular made using elevator components and operated by buttons similar to a normal elevator. The inclined elevator's

features are restricted by the European Community Standard, which is currently under discussion. This standard will guide the relationship between elevator speed and carrying capacity. For instance, a 100-passenger carrier is allowed to travel at 3.6 km/h, a 75-passenger carrier at 9km/h, and a 40-passenger carrier at 14.4 km/h. These are the maximum speeds allowed, factoring in acceleration and deceleration at each station. The actual average speed is much slower, especially for short elevators with many stops.

Meanwhile, this study addresses the dynamic change in mass that is significantly impacts the system's control and stability as highlighted in Figure 1. Properly accounting for this variable is essential for ensuring effective control strategies, especially in water-powered funiculars, where system performance depends heavily on precise mass adjustments to maintain balance and motion efficiency.

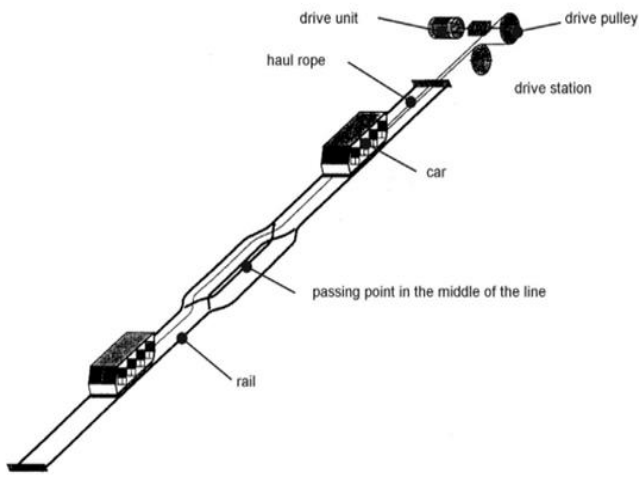


Figure 1. Layout a reversible funicular [3]

## 2. RELATED WORKS

### 2.1 Water-powered funicular train

The Lynton and Lynmouth Cliff Railway as shown in Figure 2 is distinctive in the UK as it operates without external electrical power, making it one of only three fully water-powered railways in the world. The elevator operates on a straightforward balancing principle. The two cars are permanently connected by hauling cables that run around a large 5 ft 6 in pulley wheel at the top and bottom of the tracks. There are four cables: two hauling cables that bear the weight of the cars and two tail balancing cables that counterbalance the weight of the hauling cables. When each car is 'docked' with full water tanks, they are in equilibrium and ready for loading. Each tank has a capacity of 700 gallons of water. As passengers board, variations are accommodated by the brakes, which secure the cars to the rails. The brakes on each car can support the weight of both fully loaded cars, and the lower car has a water-operated locking device that secures the car to the bottom station [4].

The impact of sudden train braking on the structural response of railway bridges under passive control is a critical consideration. A magnetorheological elastomeric bearing (MRB) with adjustable mechanical parameters was designed, tested, and modelled to address this issue by analyzing the braking dynamics of the train-bridge vibration system. Using

MATLAB, a longitudinal vibration control system simulation under train braking conditions was conducted. The results indicated that different braking positions had a significant impact on the vibration isolation system, with the most drastic structural response occurring when the train stopped at the third span. Through the proposed HSIC intelligent isolation system, the bridge beam displacement and pylon peak shear force were reduced by 53.8% and 34.4% [5].

Funicular railway tracks typically feature a bend-shaped intersection point with a specific radius as shown in Figure 3. In a previous study, Hur et al. [6] introduced a novel approach to estimating the bend radius of the curved track section (funicular track intersection point). This method involves analyzing the relative displacement between the body and the bogie when the train traverses a bend. To validate this approach, vehicle dynamics simulations and real vehicle testing were conducted on the test track. The results confirmed the effectiveness of the method, particularly when coupled with active control technology [6, 7].



Figure 2. The Lynton and Lynmouth Cliff Railway car operates without electrical power and fuel [4]

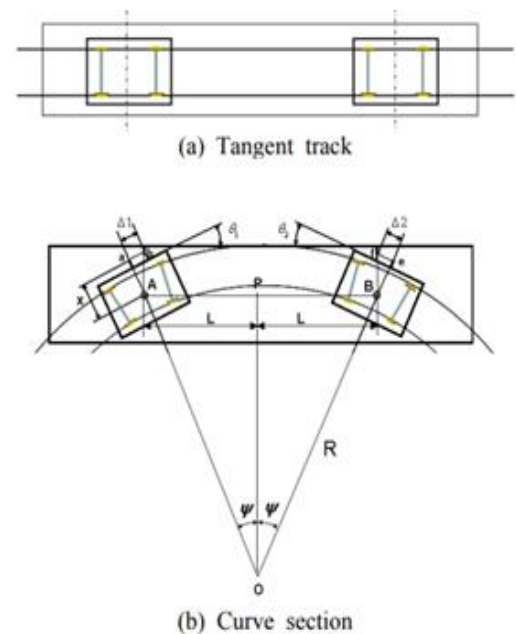


Figure 3. Relative displacement and angle between body and bogie [6]

### 3. METHODOLOGY

#### 3.1 Dynamic analysis on quarter-model vehicle

Numerous researchers have focused on analyzing the comfort and vibration of railway vehicles by developing and simulating models with various suspension configurations and degrees of freedom. For instance, Stribersky et al. [8] constructed a mathematical model of a railway vehicle using an active system to prevent rollover with the Simpack program, and then compared the simulation results with a prototype vehicle's test results. In a separate study, Kondo and Yamazaki [9] utilized computer simulation and connected computing technology to assess the kinematic performance of each bogie in a metro transportation system. They also estimated the tensile stress on the wheel axle for the direction used by modeling a single bogie in the Simpack program [9].

In a study by Jeong et al. [10], the objective was to design a bogie for a tram vehicle that could navigate a curve with a radius of 25 m while reaching a speed of 200 km/h in the city. They conducted real vehicle tests and also created a virtual model using the Adams Rail program to assess the dynamic characteristics, comfort, and safety performance of a 5-car vehicle integrated with 5 bogies featuring 10 traction motors [10]. Zhang et al. [11] developed a comprehensive model of the connection dynamics between trains and rails. This model simulated the contact zone of wheels and rails, train structure, pantograph electrical system, and airflow at high speeds. The study also reviewed the advantages and disadvantages of wheel-track contact [11].

The study of dynamic analysis on quarter model vehicle chassis, which also applies to railway bogies, has been extensively conducted using simulation software [12, 13]. Sulaiman et al. [14] utilized MATLAB Simulink to simulate quarter vehicles and employed the Semi-Active Damping Force Estimator (SADE) controller. The simulation involved inputting road conditions in the form of disturbances on the undamped mass, with mound heights (speed bump) of 0.08, 0.1, and 0.12 m and a length of 10 m. The vehicle speed was maintained at 40, 50, and 60 km/h, reflecting the speed of heavy vehicles in urban areas in Malaysia, which does not exceed 60 km/h [15].

#### 3.2 Problem formulation of water-powered funicular train

A novel vehicle system utilizing gravitational potential energy is presented. The system consists of two passenger cars connected by a steel cable on an inclined rail track. The steel cable is wound around a pulley that is driven by a motor and gearbox. Unlike an inclined lift, the driving motor in this system releases the car through the steel cable rather than pulling the load. The funicular train system involves a difference in mass between the upper and lower train cars. The upper train car, carrying a full water tank, has a greater mass than the lower train car, which carries an empty water tank. This difference in mass causes the pair of train cars to move up and down along the rail track, which has a constant railway gradient.

The mass of the carriage when it is not carrying any load is denoted as "ms." This mass includes the combined weight of the carriage itself, the passengers, and any water present. What makes this vehicle unique is that as the carriage descends from above, water is continuously released from the reservoir throughout the entire journey, until the reservoir is completely

emptied by the end of the trip. Furthermore, the cable drive pulley is intricately linked to the rate of water discharge, creating an adaptive braking system that effectively maintains a constant speed for the vehicle.

When the train is moving upward, the total mass (ms) remains constant, comprising the combined mass of the train body, passengers, and the empty reservoir. However, when the train is moving downward, the total mass (ms\*) is not constant because the water in the reservoir decreases due to unsteady flow.

The rate at which the water mass in the reservoir of a moving train carriage decreases can be described using the continuity equation for unsteady flow conditions.

$$0 = \frac{dM}{dt} = \frac{\partial}{\partial t} \int_v \rho dv + \int_A \rho \cdot V \cdot dA \quad (1)$$

$$0 = \rho \frac{\partial v}{\partial t} + \rho \cdot V \cdot A \quad (2)$$

$$\frac{\partial m}{\partial t} = -\rho \cdot V \cdot A = -\rho \cdot A \cdot \sqrt{2 \cdot g \cdot H} \quad (3)$$

$$\int \partial m = -\rho \cdot A \cdot \sqrt{2 \cdot g \cdot H} \int \partial t$$

$$m_s^* = m_s + m_w - \rho \cdot A \cdot \sqrt{2 \cdot g \cdot H} \int \partial t \quad (4)$$

If the train's speed is  $v=2 \text{ km/h}=0.55 \text{ m/s}$  and the length of the rail track is  $S=100 \text{ m}$ , then the time required for the journey can be calculated as  $t=S/v$ , which equals  $(100 \text{ m}: 0.55 \text{ m/s})=182 \text{ s}$ .

$$m_s^* = m_s + m_w - \rho \cdot A \cdot \sqrt{2 \cdot g \cdot H} \int_{t=0}^{t=182s} \partial t \quad (5)$$

After setting the initial conditions to zero, the Eqs. (1) and (2) can be transformed using the Laplace transform as described by Nugroho et al. [16].

$$[m_s s^2 + c_s s + k_s] x_2(s) = (c_s s + k_s) x_1(s) \quad (6)$$

$$\begin{aligned} [m_u s^2 + c_s s + k_t + k_s] x_1(s) \\ = k_t(s) x_{in} + (c_s s + k_s) x_2(s) \end{aligned} \quad (7)$$

By using the transposition of  $x_1(s)$  in the equation above, it becomes:

$$x_1(s) = \frac{m_s s^2 + c_s s + k_s}{(c_s s + k_s)} x_2(s) \quad (8)$$

and producing the equation:

$$\begin{aligned} m_u s^2 + c_s s + k_t \frac{m_s s^2 + c_s s + k_s}{(c_s s + k_s)} x_2(s) \\ = k_t(s) x_{in} + (c_s s + k_s) x_2(s) \end{aligned} \quad (9)$$

Then the transfer function of the vehicle body displacement is:

$$\frac{x_2(s)}{x_{in}(s)} = \frac{c_s k_t + k_s}{m_u m_s s^4 + (m_s + m_u) c_s s^3 + [(k_t + k_s) m_s + m_u k_s] s^2 + c_s k_t s + k_t k_s} \quad (10)$$

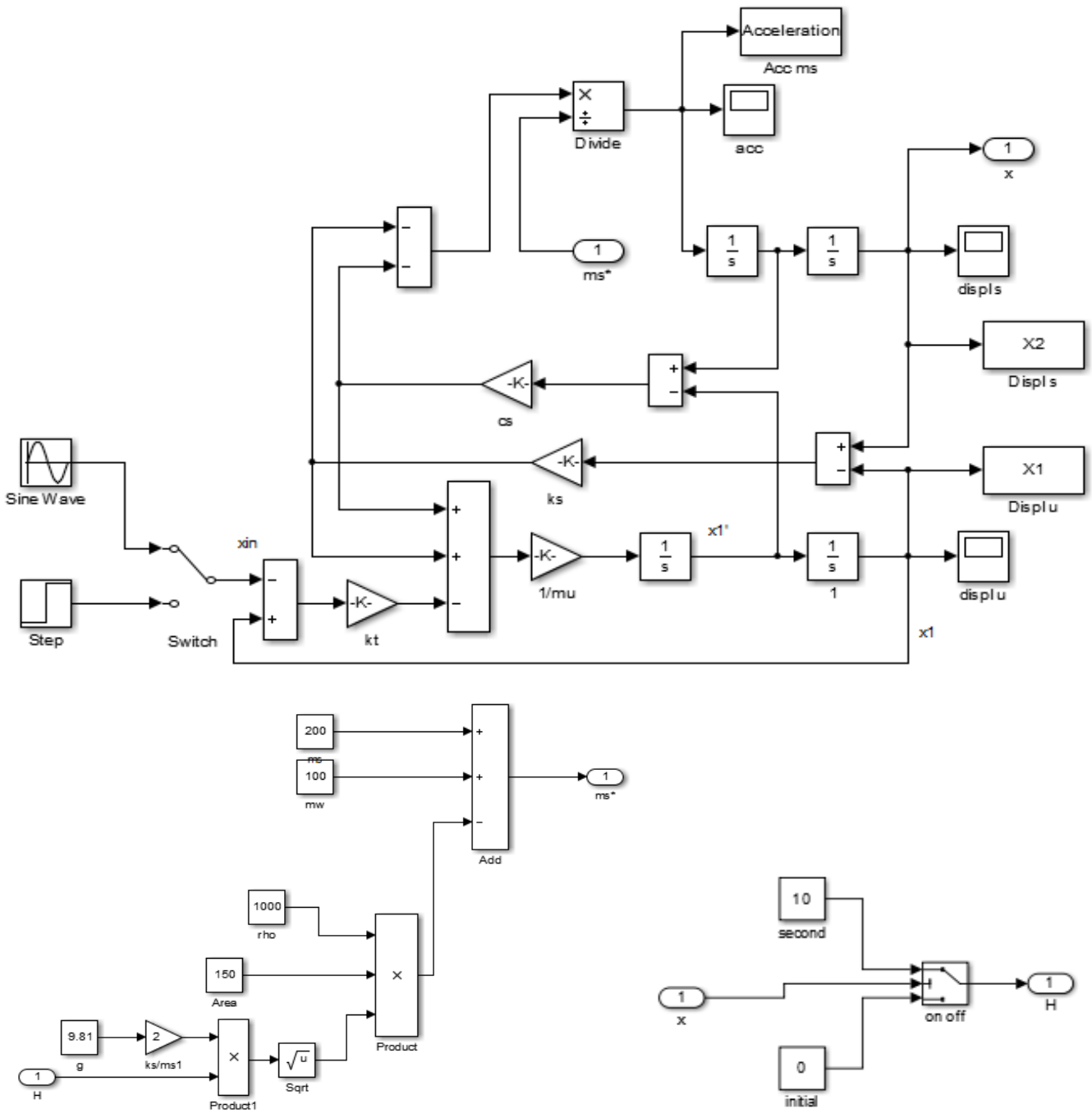
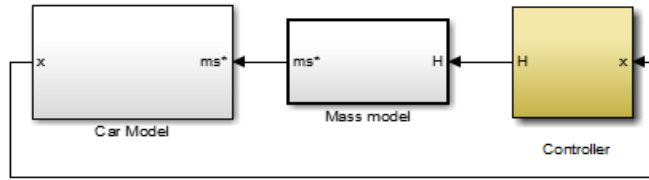


**Figure 4.** The Quarter funicular vehicle block diagram control model

In the same way, the transfer function of the unsprung mass (wheel) is obtained:

$$\frac{x_1(s)}{x_{in}(s)} = \frac{m_s s^2 + c_s s + k_s}{(c_s s + k_s) \frac{m_u m_s s^4 + (m_s + m_u) c_s s^3 + [(k_t + k_s) m_s + m_u k_s] s^2 + c_s k_t s + k_t k_s}{c_s k_t + k_s}} \quad (11)$$

In Eq. (11), the vehicle's vibration response is represented as the displacement amplitude ( $x_1$  and  $x_2$ ) in response to variations in the road or rail surface ( $x_{in}$ ). Experimental data, including the mass of the vehicle/passenger/water ( $m_s$ ), spring constant ( $k_s$ ), and damping constant ( $c_s$ ), is processed and simulated in the Simulink Matlab program to analyze the vehicle's vibration response under two types of road profiles: step and sine. Below is the Simulink diagram depicting the setup.

### 3.3 Active suspension control of quarter-model system

A linear quadratic regulator (LQR) controller has been proposed by Bezabh [17] for implementation in the active suspension system and compared it with the passive suspension system. This study aimed to simulate and analysis of the vehicle performance by constructing a MATLAB/SIMULINK on a quarter automobile model. The results showed that the performance of the passive suspension system and the LQR controller are contrasted. The simulation's findings demonstrated how the LQR controller enhances ride comfort and wheel deflection in automobile suspension systems at all road inputs even at high vehicle speeds the LQR controller helps the system for better ride comfort of the passengers and helps the system to better the life of the vehicle.

Control systems based on fuzzy logic (FL) and proportional-integral-derivative (PID) has also been applied to vehicle suspension to evaluate driving comfort performance by Ab Talib et al. [18]. An experimental quarter vehicle test rig complete with a magnetorheological (MR) damper was used in this study to test and compare the effectiveness of the proposed FL-AFA and PID-AFA controllers against the passive controller system. The experiment result indicated that the PID-AFA shows a good response compared to the FL-AFA and the passive system, with the ability to reduce the vibration amplitude by up to 57.1%.

In this article, the funicular railway car dynamical system with mass control is mathematically represented as the vehicle's quarter-model, illustrated as a block diagram in Figure 4. This representation is based on Newton's second law model, as shown in Figure 5.

$$m_s \ddot{x}_2 + c_s(\dot{x}_2 - \dot{x}_1) + k_s(x_2 - x_1) = 0 \quad (12)$$

$$m_u \ddot{x}_1 + k_t(x_1 - x_{in}) + c_s(\dot{x}_1 - \dot{x}_2) + k_s(x_1 - x_2) = 0 \quad (13)$$

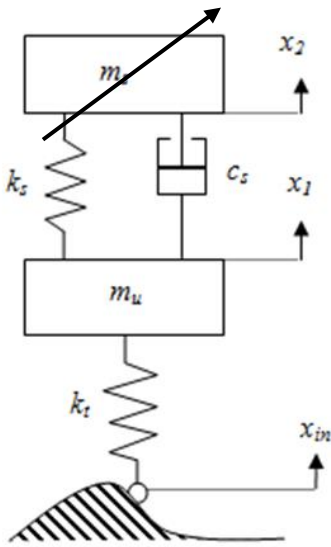


Figure 5. The Quarter model of a car with two degrees of freedom (DOF) [19]

### 3.4 The proposed conceptual design funicular train

The study introduces a novel vehicle system that operates on gravitational potential energy. It consists of two passenger cars connected by a steel cable on an inclined rail track. The

steel cable is wrapped around a pulley driven by a motor and gearbox. Unlike an inclined lift, this funicular vehicle system releases the car through the steel cable, in contrast to the driving motor's function of pulling the load through the cable in an inclined lift.

In the funicular train system, there is a difference in mass between the upper and lower train cars. The upper train that will move down has a greater mass than the lower train car because the upper part carries a full water reservoir while the lower train does not bring water. In Figure 6, the water reservoir placed in the bottom of the car that will continuously waste the water as long as the track. The lower part carries an empty water reservoir so the difference in mass of the two train cars causes the movement of a pair of train cars up and down following the rail track which has a constant angle of inclination as Eq. (5).

The car's load capacity is measured in metric tons and encompasses the combined mass of the vehicle's body, passengers, and water. What sets this vehicle apart is that as it descends from above, the reservoir continuously releases water throughout the journey, emptying completely by the trip's end. The cable drive pulley is intricately linked to the rate of water discharge, forming an adaptive braking system that maintains the vehicle's speed at a constant level.

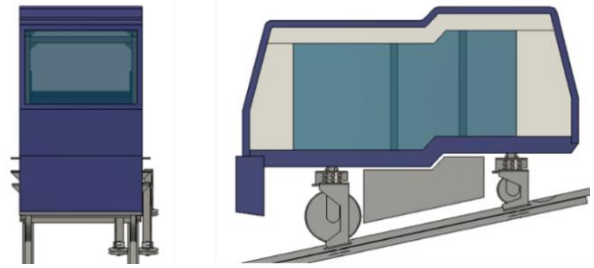


Figure 6. Design body of funicular railway train with reservoir tank water in the bottom floor

## 4. RESULT AND DISCUSSION

In this section, simulation tests are conducted using two types of inputs that are bump input and sine input, to evaluate the performance of the suspension systems under different operating conditions. Bump input assesses the system's ability to handle transient responses, including peak amplitude and settling time, which are critical for passenger comfort. Meanwhile, sine input tests the system's steady-state response, highlighting its ability to manage repeated forces without amplifying vibrations.

### 4.1 Performance under simulation bump input

The bump input simulates sudden, sharp disturbances, such as encountering a track irregularity, pothole, or abrupt elevation changes.

In Figure 7 and Table 1, both graphs demonstrate a similarity in the displacement response of the sprung mass or vehicle body to Bump Input. This can be attributed to the fact that it takes approximately 5.2 seconds to reach the steady state condition. The rise time, which represents the duration of the displacement wave generated by the suspension, falls between 0.1 and 0.5 seconds.

Based on Figure 8 and Table 2, both graphs exhibit a resemblance in the acceleration response of the sprung mass

or vehicle body to bump input. This similarity arises from the fact that it takes only about 2 seconds to reach the steady state condition. Additionally, the rise time, which represents the duration of the vibration wave generated by the suspension, falls within the range of 0.1 to 0.2 seconds.

**Table 1.** Vehicle body displacement for bump input

No.	Characteristics	Symbol	Values
1	Rise Time	tr	0.1-0.5s
2	Maximum Amplitude	MP	0.19 mm
3	Peak Amplitude	AP	0.18 mm
4	Steady State	SS	5.2s

In both Figure 9 and Table 3, the graphs demonstrate the identical acceleration response of unsprung mass or tire with a step function. This similarity arises from the fact that it takes only approximately 0.5 seconds to reach the steady state condition. The rise time, which denotes the duration of the

displacement wave generated by the suspension, falls within the range of 0 to 0.1 seconds.

**Table 2.** Vehicle body acceleration for bump input

No.	Characteristics	Symbol	Values
1	Rise Time	tr	0.1-0.4 s
2	Maximum Amplitude	MP	3.5 m/s <sup>2</sup>
3	Peak Amplitude	AP	-0.2 m
4	Steady State	SS	2 s

**Table 3.** Unsprung mass acceleration for bump input

No.	Characteristics	Symbol	Values
1	Rise Time	tr	0-0.1s
2	Maximum Amplitude	MP	9.6 m/s <sup>2</sup>
3	Peak Amplitude	AP	-0.8 m/s <sup>2</sup>
4	Steady State	SS	0.1s

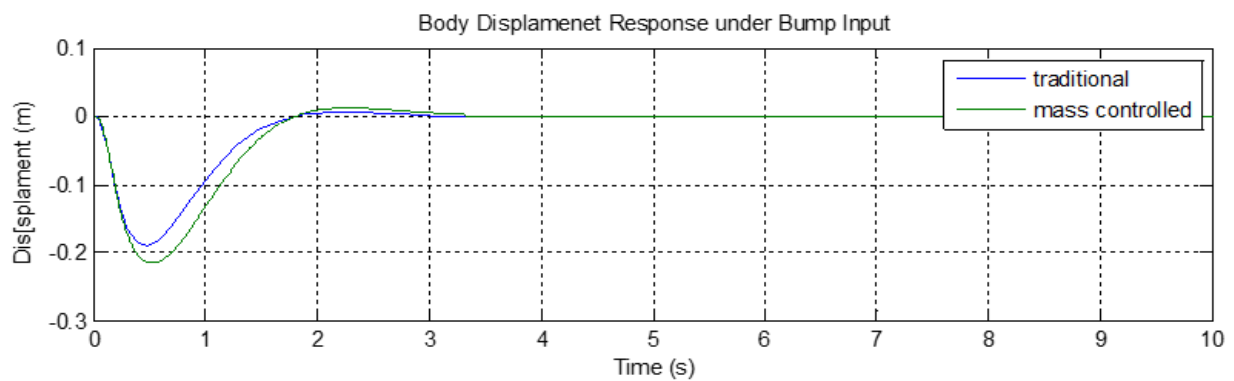


**Figure 7.** Body displacement response under bump input diagram

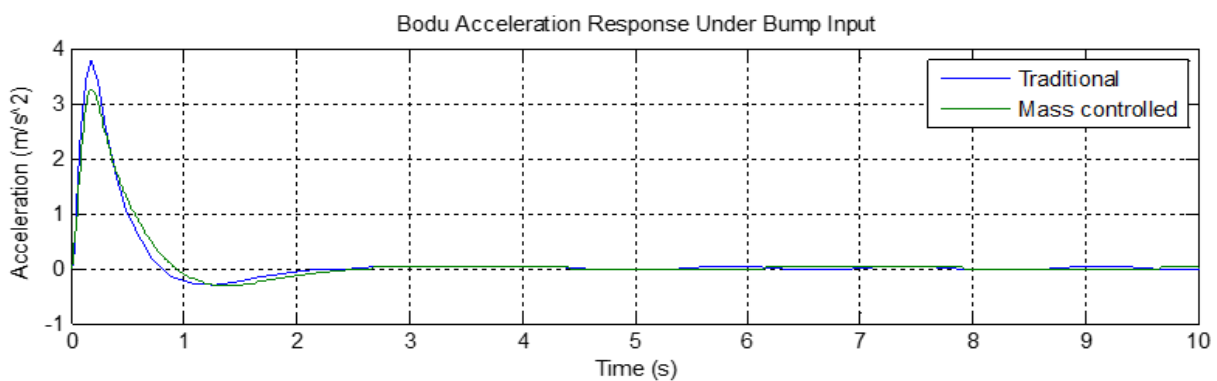


**Figure 8.** Body displacement response under bump input diagram

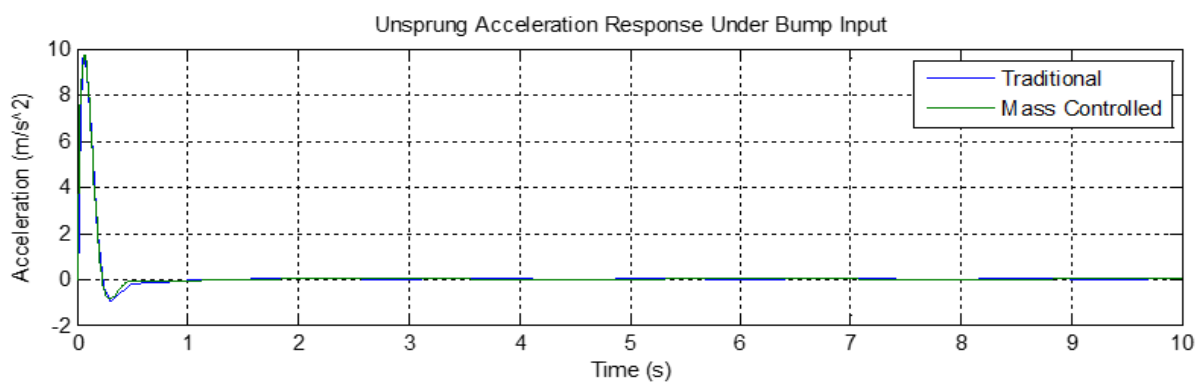


**Figure 9.** Unsprung acceleration response under bump input diagram

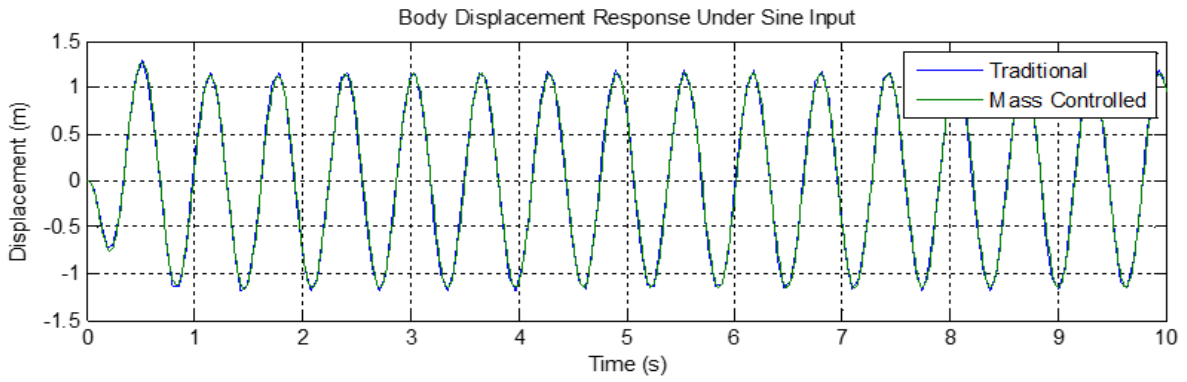


**Figure 10.** Body displacement response under sine input diagram

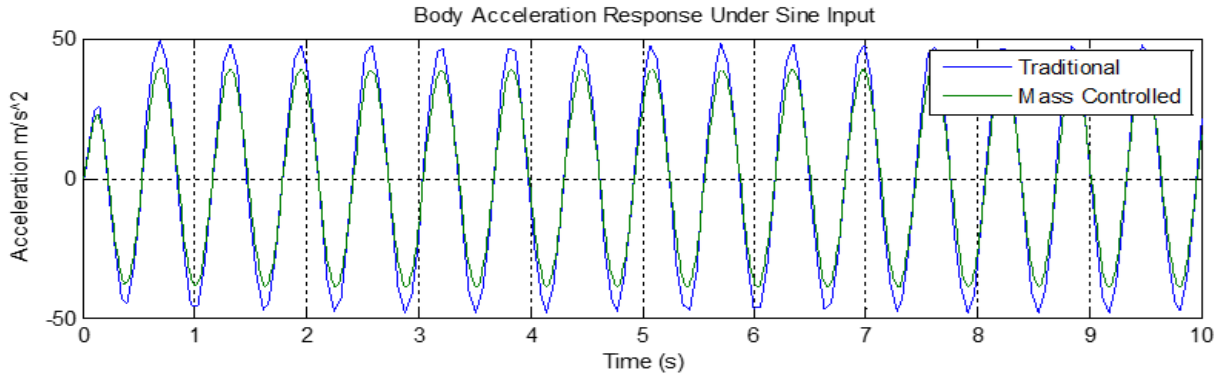


**Figure 11.** Body acceleration response under sine input diagram

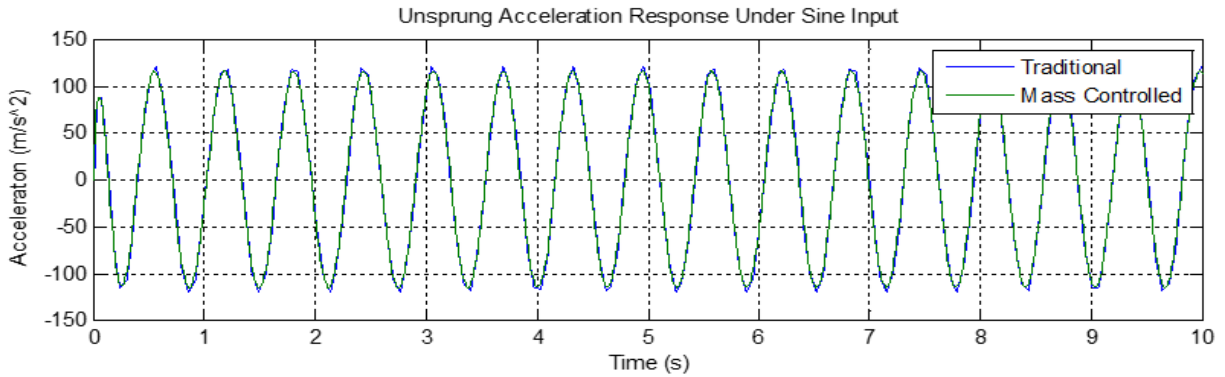


**Figure 12.** Unsprung acceleration response under sine input diagram

**Table 4.** Vehicle body displacement for sine input

No.	Characteristics	Symbol	Values
1	Rise Time	tr	0.3-0.6 s
2	Maximum Amplitude	MP	1.2 m
3	Peak Amplitude	AP	1.2 m
4	Steady State	SS	0.8 s

#### 4.2 System performance under operating condition of sine input

The sine input represents periodic disturbances, such as oscillations caused by uneven tracks over time.

As shown in Figure 10 and Table 4, both graphs demonstrate the identical displacement response of the sprung mass or vehicle body to a sine input. This similarity is due to the short time, approximately 0.86 seconds, required to reach the steady-state condition. The rise time, representing the

duration of the displacement wave generated by the suspension, falls between 0.3 seconds and 0.61 seconds.

**Table 5.** Vehicle body acceleration for sine input

No.	Characteristics	Symbol	Values
1	Rise Time	tr	0.1-0.8s
2	Maximum Amplitude	MP	10 mm
3	Peak Amplitude	AP	10 mm
4	Steady State	SS	1.8 s

**Table 6.** Unsprung mass acceleration for sine input

No	Characteristics	Symbol	Values
1	Rise Time	tr	0.1-0.8s
2	Maximum Amplitude	MP	1.5 mm
3	Peak Amplitude	AP	1.5 mm
4	Steady State	SS	2.6 s

In Figure 11 and Table 5, both graphs demonstrate a similarity in the Acceleration Response of the sprung mass or vehicle body to a Sine Input. This is due to the relatively short time it takes to reach the steady state condition, which is approximately 1.8 seconds. The rise time, representing the duration of the vibration wave produced by the suspension, falls between 0.1 and 0.8 seconds.

Based on Figure 12 and Table 6, both graphs display identical Acceleration Response to Sine Input. This similarity arises from the short time it takes to reach the steady state condition, which is approximately 2.6 seconds. The rise time, representing the duration of the displacement wave generated by the suspension, ranges from 0.1 seconds to 0.8 seconds.

## 5. CONCLUSIONS

The results of this study show no significant difference in acceleration, displacement, responsiveness, stability, and suspension waves between the traditional upward train system and the controlled mass downward train system, which discharges water from a tank on the bogie in an unsteady flow manner. For example, the input in the form of a bump profile has almost the same value in a rise time of around 0.2-0.3 seconds, a maximum amplitude of around 0.2 m, a peak amplitude of around 0.22 m and a steady state of around 5.2 seconds.

This is because the speed of water discharge has been synchronized with the speed of the vehicle. As the funicular moves downward from the upper station, the water tank is full, and when the vehicle reaches the lower station, the water tank is empty. This demonstrates that the adaptive braking system, which discharges water in a controlled manner, effectively prevents shock acceleration and deceleration. The conclusion of the funicular train dynamics simulation test using adaptive water discharge braking is as expected.

The analysis using Simulink in MATLAB reveals distinct differences between the traditional upward train suspension system and the controlled mass downward train system with active suspension control. The controlled mass downward train system exhibits a lower maximum amplitude compared to the traditional system. This reduction is due to the active suspension system effectively absorbing external forces and disturbances, thereby mitigating excessive oscillations and vibrations.

As for the future works, there is a need for experimental validation of this study to measure the effectiveness and applicability of the developed mass adaptive control method. For this purpose, a quarter-car active suspension test-rig driven by an electro-hydraulic actuator will be developed.

## AUTHOR CONTRIBUTIONS

This manuscript has been compiled in collaboration with multiple authors. The following contributors from each author using the initial name are: Conceptualization, methodology, formal analysis, writing-original draft preparation, B.W. and P.W.N.; Software, visualization and validation, P.W.N., A.F., H.W.; Data curation and formal analysis, P.W.N.; Supervision, writing-review and editing, S.S., M.A.N. and N.S.M.N.; Project administration, P.W.N; Funding acquisition, B.W.; All authors have read and agreed to the published version of the manuscript.

## ACKNOWLEDGMENT

The authors wish to thank the Directorate General of the Vocational Education (DAPTV) Ministry of Education and Culture of the Republic of Indonesia for the financial support under the grant number 273/PKS/D.D4/PPK.01.APTV/VII/2024. Special appreciation to State Polytechnic Malang (Polinema) and Universiti Teknologi Malaysia (UTM) for the continuous supports between both institutes.

## REFERENCES

- [1] Nam, D.H., Huh, H.M., Lee, J.S. (2012). Environmental benefit analysis for railroad-related projects. *Journal of the Korean Society for Railway*, 15(2): 179-184. <https://doi.org/10.7782/jksr.2012.15.2.179>
- [2] Albertus, R. (2023). Collaborative governance tourism transportation development in Post Covid-19. In *International Conference of Public Administration and Governance (ICOPAG 2022)*, Atlantis Press, pp. 324-340. [https://doi.org/10.2991/978-2-38476-082-4\\_30](https://doi.org/10.2991/978-2-38476-082-4_30)
- [3] Hoffmann, K., Liehl, R. (2005). Cable-Drawn urban transport systems. *Urban Transport, WIT Transactions on the Built Environment*, 77.
- [4] Cooper, D.A. (2014). The four remaining water balance lifts in the UK. In *4th Symposium on Lift and Escalator Technologies*, 4(1): 45-55. [https://liftescalatorlibrary.org/paper\\_indexing/papers/0000072.pdf](https://liftescalatorlibrary.org/paper_indexing/papers/0000072.pdf).
- [5] Li, R., Zhou, H., Wu, Y., Wang, X. (2016). Human-simulated intelligent control of train braking response of bridge with MRB. In *Active and Passive Smart Structures and Integrated Systems 2016*, pp. 844-854. <https://doi.org/10.1117/12.2218869>
- [6] Hur, H.M., Park, J.H., You, W.H. (2012). Curvature estimation method of curve section using relative displacement between body and bogie of rolling-stock. *Transactions of the Korean Society of Mechanical Engineers A*, 36(11): 1479-1485. <http://doi.org/10.3795/KSME-A.2012.36.11.1479>
- [7] Sim, K.S., Hur, H.M., Song, H.S., Park, T.W. (2014). Study of the active radial steering of a railway vehicle using the curvature measuring method. *Journal of Mechanical Science and Technology*, 28: 4583-4591. <https://doi.org/10.1007/s12206-014-1026-1>
- [8] Stribersky, A., Rulka, W., Netter, H., Haigermoser, A. (1997). Modeling and simulation of advanced rail vehicles. *IFAC Proceedings Volumes*, 30(8): 473-478. [https://doi.org/10.1016/S1474-6670\(17\)43866-3](https://doi.org/10.1016/S1474-6670(17)43866-3)
- [9] Kondo, O., Yamazaki, Y. (2013). Simulation technology for railway vehicle dynamics. *Nippon Steel & Sumitomo Metal Technical Report*, 105: 77-83.
- [10] Jeong, N.T., Wang, M., Yoo, S., Kim, W.K., Han, S.Y., Lee, H.Y., Suh, M.W. (2017). Conceptual design of high-speed semi-low-floor bogie for train-tram. *International Journal of Automotive Technology*, 18: 523-533. <https://doi.org/10.1007/s12239-017-0052-2>
- [11] Zhang, S., Zhang, W., Jin, X. (2007). Dynamics of high speed wheel/rail system and its modelling. *Chinese Science Bulletin*, 52(11): 1566-1575. <https://doi.org/10.1007/s11434-007-0213-1>
- [12] Vaishnav, A., Sarvaiya, M., Dhabaliya, P., Rajguru, S.

- (2016). Mathematical modelling and comparison of two degree of freedom suspension system of quarter car. *Imperial Journal of Interdisciplinary Research*, 2(11): 128-137. <https://www.researchgate.net/publication/308884979>.
- [13] Kanchwala, H., Chatterjee, A. (2017). A generalized quarter car modelling approach with frame flexibility and other nonlocal effects. *Sādhanā*, 42: 1175-1192. <https://doi.org/10.1007/s12046-017-0675-z>
- [14] Sulaiman, S., Samin, P.M., Jamaluddin, H., Rahman, R.A., Abu Bakar, S.A. (2015). Ground semi active damping force estimator (gSADE) for magnetorheological damper suspension system using quarter heavy vehicle model. *Applied Mechanics and Materials*, 789: 913-917. <https://doi.org/10.4028/www.scientific.net/AMM.789-790.913>
- [15] Wu, Y., Zeng, J., Shi, H., Zhu, B., Wang, Q. (2022). A hybrid damping control strategy for high-speed trains running on existing tracks. *Journal of Low Frequency Noise, Vibration and Active Control*, 41(3): 1258-1271. <https://doi.org/10.1177/14613484221087513>
- [16] Nugroho, P.W., Li, W., Du, H., Alici, G., Yang, J. (2014). An adaptive neuro fuzzy hybrid control strategy for a semiactive suspension with magneto rheological damper. *Advances in Mechanical Engineering*, 6: 487312. <https://doi.org/10.1155/2014/487312>
- [17] Bezabh, W.W. (2023). Quarter car suspension system modelling, simulation, and performance analysis under dynamic conditions, PREPRINT (Version 1) Research Square. <https://doi.org/10.21203/rs.3.rs-3730685/v1>
- [18] Ab Talib, M.H., Mat Darus, I.Z., Mohd Samin, P., Mohd Yatim, H., Hadi, M.S., Shaharuddin, N.M.R., Mazali, I.I., Ardani, M.I., Mohd Yamin, A.H. (2023). Experimental evaluation of ride comfort performance for suspension system using PID and fuzzy logic controllers by advanced firefly algorithm. *Journal of the Brazilian Society of Mechanical Sciences and Engineering*, 45(3): 132. <https://doi.org/10.1007/s40430-023-04057-5>
- [19] Na, J., Huang, Y., Wu, X., Liu, Y. J., Li, Y., Li, G. (2021). Active suspension control of quarter-car system with experimental validation. *IEEE Transactions on Systems, Man, and Cybernetics: Systems*, 52(8): 4714-4726. <https://doi.org/10.1109/TSMC.2021.3103807>

## NOMENCLATURE

$m_s$	vehicle sprung mass (when the train is moving upward) [kg]
$m_s^*$	vehicle sprung mass (when the train is moving downward) [kg]
$m_w$	mass of water in the reservoir when the train is moving downward [kg]
$\rho$	density of water (1000 kg/m <sup>3</sup> )
$A$	cross-sectional area of the reservoir's outlet hole [m <sup>2</sup> ]
$g$	acceleration due to gravity (9.81 m/s <sup>2</sup> )
$H$	water level relative to the outer hole position in the reservoir [m]
$T$	time taken based on train speed [sec]
$m_u$	mass of the vehicle wheel (kg)
$c_s$	suspension damper constant (kg/s)
$k_s$	suspension spring stiffness constant (kg/s <sup>2</sup> )
$k_t$	wheel stiffness constant (kg/s <sup>2</sup> )
$x_1$	displacement of $m_u$ (m)
$x_2$	displacement of $m_s$ (m)
$x_{in}$	road surface profile (m)